national accelerator laboratory

TM-194
0423

DESIGN OF MAIN RING BENDING MAGNETS FOR IMPROVED HIGH FIELD PERFORMANCE

G. McD. Bingham

December 5, 1969

Introduction

The Main Ring of the NAL accelerator uses two bending magnets, B1 and B2, in its separated function lattice. The nominal aperture of B1 is 5 in. x 1.5 in. and that of B2 is 4 in. x 2 in. Lari and Teng[1] have published designs obtained by use of the computer program TRIM. Their designs have the advantages of good field uniformity over ∿ 80% of the nominal aperture and minimal saturation effects for fields up to ∿ 20 kg. The designs have the disadvantages that crenellation is required at higher fields and also that close proximity of the inner conductors to the good field region requires that these conductors be accurately located. For example, there is a tolerance of ± 0.005 in. on the average midplane gap between the inner conductors.

The work described in this report was undertaken in an effort to improve the high field performance of the two bending magnets. At the same time, we would like to increase the distance of the inner conductors from the center, if possible. We have used the computer program LINDA[2].

Design Input Data

Parameter	B1	B2
Nominal Aperture	5 in x 1-1/2 in	4 in x 2 in
Turns	12	16
Outer Yoke Dimensions	width 25-1/4 in height 14-1/4 in	width 25-1/4 in height 14-1/4 in
Stacking factor	0.99	0.99
Overall area per Conductor (outer) (inner)	1.01 in^2 $\sim$0.9 in^2	1.01 in^2 1.01 in^2
Minimum clearances		
cond to cond	.030 in	.030 in
cond to grnd	.085 in	.085 in
Coil Configuration	2 outers, 1 inner	2 outers, 1 inner
Good Field $K=\frac{B'}{B}$	$\lvert K\rvert < 0.01\ m^{-1}$	$\lvert K\rvert < 0.01\ m^{-1}$

Table 1. Design Parameters for B1 and B2 Magnets

The design parameters are listed in Table 1. The apertures and turns are discussed in reference 3. Since B1 and B2 magnets will be connected in series, it is necessary that their fields "track". Calculations[4] indicate an excursion of 1.5 cm in the equilibrium orbit for a 1% B1 - B2 field difference. Thus the tracking error should be <<1% at low fields. The outer yoke dimensions are strongly influenced by engineering and economic considerations. The values listed in Table 1 have evolved in a manner which has not always been clear. The stacking factor has been taken from measurements[5] performed on model magnets. The conductor

area and good field criterion come largely from reference 3. The coil configuration was chosen in an attempt to minimize costs[6]. For the same reason, a coil of large cross-section conductor is favored over parallel coils of smaller cross-section conductor.

In order to calculate the magnet performance, especially at high fields, it is necessary to know the B-H curve of the steel which is to be used. Tests[7] have been made on sample low carbon steel supplied to NAL by the steel vendors. The B-μ-H values are given in Table 2 under the heading "TEST". In order to demonstrate the effect of variations in μ we have also done calculations using the decarburized steel table contained in the LINDA program. B-μ-H results for this steel are given under the heading "LINDA" in Table 2. Note that we have not bothered to round off the numbers in Table 2. Recent CERN results[8] up to 20 kgauss are in agreement (within few percent) with the table in LINDA, excepting at very low fields where LINDA uses a straight line for simplicity, since the low field μ values do not influence the field shape at the fields considered in this work. From Table 2 it is apparent that the test steel μ values show a marked "bump" relative to the Linda steel μ values in the range ∿ 20-22 kgauss. In fact some of the test steel results fall above the tabulated results for pure iron[9] in this region. It would therefore seem wise to treat them with some caution until they can be rechecked. They have been included

L I N D A			T E S T		
B(TESLAS)	MU	H(OERS)	B(TESLAS)	MU	H(OERS)
0.	4444.44	0.	0.	7246.38	0.
1.2000	3246.75	3.696	1.0000	7246.38	1.380
1.4000	2222.22	6.300	1.0500	7241.13	1.450
1.5000	1499.25	10.005	1.1000	7097.23	1.550
1.5500	1069.52	14.492	1.1500	6887.05	1.670
1.6000	709.22	22.560	1.2000	6666.67	1.800
1.6500	458.72	35.970	1.2500	6345.18	1.970
1.7000	308.64	55.080	1.3000	5910.17	2.200
1.7500	230.41	75.950	1.3500	5509.64	2.450
1.8000	176.37	102.060	1.4000	4516.71	3.100
1.8500	139.08	133.015	1.4502	3222.69	4.500
1.9000	111.11	171.000	1.5000	2418.96	6.201
1.9500	90.09	216.450	1.5502	1291.99	11.998
2.0000	75.19	266.000	1.6000	727.27	22.000
2.0500	60.98	336.200	1.6502	445.83	37.013
2.1000	49.50	424.200	1.7000	309.12	54.995
2.1250	44.25	480.249	1.7501	224.42	77.986
2.1500	39.06	550.400	1.8000	171.41	105.012
2.1750	33.00	659.025	1.8501	140.19	131.970
2.2000	26.53	829.400	1.9000	117.30	161.975
2.2500	18.00	1249.987	1.9501	101.60	191.951
2.2797	15.00	1519.780	2.0000	89.29	224.000
2.3069	13.00	1774.505	2.0501	79.74	257.085
2.3443	11.00	2131.179	2.1002	71.94	291.933
2.3996	9.00	2666.176	2.1501	59.74	359.929
2.4905	7.00	3557.854	2.2000	38.26	575.080
2.5627	6.00	4271.207	2.2501	22.50	999.949
2.6706	5.00	5341.198	2.3000	15.65	1469.700
2.8498	4.00	7124.531	2.4000	9.76	2460.000
3.2074	3.00	10691.094	2.5000	7.35	3400.000
3.5644	2.50	14257.630	3.0000	3.57	8400.000
4.2782	2.00	21391.201	4.0000	2.19	18296.000
4.8134	1.80	26740.948			
5.7052	1.60	35657.332			
6.4186	1.50	42790.467			
7.4887	1.40	53490.838			
9.2721	1.30	71323.907			
10.6989	1.25	85591.028			
12.8389	1.20	106990.291			
23.5390	1.10	213990.594			

Table 2. B-μ-H tables for Linda steel and Test steel.

in the work of this report in order to facilitate comparison of our design with other designs which also have used the test steel μ values.

Calculations assuming a stacking factor of 0.96 have also beem made to show the effect of this parameter. Thus we have calculated 3 cases in all for both B1 and B2, with the steel and stacking factor assumptions set out in Table 3.

Case	Stacking Factor	Type of Steel
1	0.99	Linda
2	0.99	Test
3	0.96	Linda

Table 3. The parameters assumed in the three cases calculated for both B1 and B2.

Design Method

As noted above, the design computations were done using the computer program LINDA. This is a two dimensional magnetostatic program with general boundaries. One may use either a built in B-H table for a good decarburized iron or an arbitrary iron magnetization curve may be input. The computer runs were made on C.D.C. 6600 machines at N.Y.U. and L.R.L.

Both our B1 and B2 designs use tapered pole tips and edge shims. We define the quantity Ampfac as:

$$\text{Ampfac} = \frac{\text{Excitation for midgap B with given iron}}{\text{Excitation for midgap B with infinite perm. iron}}$$

The advantage of tapering the pole tip is that the leakage flux is reduced. This results in less saturation of the magnet at a given midgap field, i.e. a lower value of Ampfac, It is particularly important for good high field performance. Tapered pole tips have appeared in the literature of magnet design for more than 30 years[10]. The advantage of edge shims is that the good field region is increased for a given magnet pole size and was first noted by Rose[11] in 1938.

Figure 1 shows the design starting point. The shim was placed at a distance of one half gap beyond the nominal aperture mainly on the basis of Figure 4 in Rose's paper. A transition of 0.2 in. (one mesh unit) was allowed on each side of the shim. The shim thickness was determined by trial and error. The distance D was chosen = (one half nominal aperture + $\sim$ 0.5 in) in an effort to move out the inner conductor. Then the coils were set up in the coil space so as to have Rs $\simeq$ Rt. The design then proceeded by trial and error to find the correct shim thickness to correct the low field K curve. The high field K curves were corrected by an appropriate combination of inner conductor position D and taper Θ. The K curve variations for these changes are sketched in Figure 2. The Ampfac values were kept as small as possible throughout the work.

The final B1 and B2 magnets are shown in Figure 3 and Figure 4 respectively. They were obtained with Linda iron, but appear to be close to optimum for Test iron also. As

can be seen from Figure 3 and Figure 4, the symmetrical H type magnets have been set up in the second quadrant. This corresponds to an MTYPE=4 magnet in the LINDA program. A mesh size of 0.2 in x 0.2 in was usually employed. Approximately 6 minutes of CDC 6600 computer time was required to run a given magnet problem for one value of the central field.

Inspection of the B1 and B2 designs shows that we have not been able to move the inner conductors away from the center to any appreciable extent. It appears that this fact is related to the somewhat restrictive outer yoke dimensions specified. Rough calculations made on a B2 magnet in which both outer yoke dimensions were increased ∿ 1/2 in. indicated that the inner conductor could be moved out to ∿ 2.3 in. which would ease the tolerance requirement by a factor ∿ 2.

Figure 5 and Figure 6 show the flux lines and potential lines for B1 and B2 respectively at 21 kgauss with Linda iron and stacking factor = 0.99, i.e. Case 1. The potential drop along the return path is smooth and there are no badly saturated areas. The increment between scalar equipotentials in the iron is 1% of the gap excitation.

Magnetic Field Gradient Results

Case 1 Stacking Factor = 0.99, Linda Iron

The midplane K curves are shown in Figure 7 and Figure 8A for B1 and B2 respectively. The good field region (± 2.25 in. for B1 at low field, ± 1.65 in. for B2 at low field)

decreases ∿ 10% B1, ∿ 8% B2 up to ∿ 20 kgauss. It then drops a further ∿ 25% for B1, ∿ 9% for B2 as the K curves rise. The K curves then change direction and fall rapidly as the field is increased further. Full aperture is available at ∿ 21.9 kgauss. Alternatively, if it was desired to have full aperture at 22.5 kgauss, then a line integral second derivative correction ($\frac{\partial^2 B}{\partial x^2}$ x path length) of ∿ 650 kgauss m^{-1} per half cell would be required. Each half cell is designed to have a one foot long sextupole capable of a maximum gradient of 2.0×10^3 kgauss m^{-2} (i.e. 600 kgauss m^{-1} per half cell) which is probably sufficient correction to maintain full aperture at 22.5 kgauss.

Also shown in Figure 7 and Figure 8A are the Ampfac values for each field. The tracking error of B1 and B2 is given by the difference in magnetic field for the two magnets at a fixed current. Figure 8B shows how the tracking error may be determined. The Ampfac values are plotted against magnetic field for each magnet. Constant current lines (hyperbolic) are drawn in the region of interest. These lines are used to determine the slope of the line P1P2 such that $\Delta B1 = -\Delta B2$. Then P1 and P2 give the operating points of B1 and B2 at the same current. For example, the tracking error at 22.5 kgauss is 0.9% which is much less than the 2.7% difference in Ampfac for the two magnets at a fixed field of 22.5 kgauss. This may be excessive. However, D. Edwards notes[4] that most of the deviation is

caused by the non-uniform distribution of B1 and B2 magnets in the regions of the long straight sections and medium straight sections. Thus installation of correction magnets in these regions only would probably allow 22.5 kgauss operation. The tracking error at fields up to ∿ 21.5 kgauss is negligible.

In our computations we have generally used a 0.2 in. x 0.2 in. mesh. The effect of changing from this mesh to a 0.1 in. x 0.1 in. fine mesh was investigated for several fields for both B1 and B2. The fine mesh results for K are shown by the dotted curves and the fine mesh Ampfac results are shown to the right of the Ampfac tables in both Figure 7 and Figure 8A. In the present work it is clear that the errors of the 0.2 in. mesh are small. Thus the use of 0.1 in. mesh for all calculations, with ∿ 4 fold increase in computer time, was not necessary.

Case 2 Stacking Factor = 0.99, Test Iron

These results are shown in Figure 9 and Figure 10. In comparison with the Case 1 results the Case 2 K curves show a larger scatter in the 20 kgauss to 21.5 kgauss region. The 20 kgauss curve moves lower while the 21.5 kgauss curve moves higher. However, the performance at the highest fields is improved. The present case also has lower Ampfac numbers than Case 1 but the tracking situation is very similar. The scatter of the K curves in the 20 kgauss-21.5 kgauss region appears to be due to the "bump" in the Test β

values in this region. The sextupole correction required for full aperture at 22.5 kgauss in Case 2 is only about half that required for Case 1.

Case 3 Stacking Factor = 0.96, Linda Iron

The K curves for this case are shown in Figure 11 and Figure 12. The high field results are now much worse. The present curves can be obtained approximately from those of Case 1 simply by estimating the position of the curve in Case 1 corresponding to a 3% increase in flux density. The importance of maintaining the highest possible stacking factor in order to achieve good high field performance is also apparent when one compares the Ampfac tables for Case 1 and the present case.

Power Requirements

The power requirements are summarized in Table 4. The results from Case 2 have been used. It has been assumed that the average conductor length per turn is 43.5 ft. and that the conductor corners have 1/16 in. radius. The resistivity used is that for 100% conductivity copper at 20°C (6.79×10^{-7} Ω in.). The resulting B1 and B2 resistances are 5.06×10^{-3} ohm and 6.19×10^{-3} ohm respectively. Since all magnets are in series and the numbers of B1 and B2 magnets are nearly equal then the current for a given average field will be the average of the B1 and B2 currents, to a good approximation. This is also apparent from Figure 8B.

Mag. Field (kgauss)	Proton Energy (GeV)	B1		B2		Average Current (Amps)	Power (kw)	
		Ampfac	Current (Amps)	Ampfac	Current (Amps)		B1	B2
9	200	1.002	2279	1.002	2274	2277	26.2	32.1
18	400	1.022	4646	1.022	4647	4647	109.3	133.7
20	444	1.059	5354	1.058	5347	5351	144.9	177.2
21	467	1.086	5762	1.081	5735	5749	167.2	204.6
21.5	478	1.105	6002	1.096	5955	5979	180.9	221.3
22	489	1.135	6310	1.119	6221	6266	198.7	243.0
22.5	500	1.178	6694	1.150	6540	6617	221.6	271.0

Table 4. B1 and B2 power requirements. The power figures are for the average current shown.

Discussion

We have shown that is is possible to design Main Ring bending magnets which maintain adequate aperture up to proton energies ∿ 500 GeV (corresponding to a magnetic field ∿ 22.5 kgauss). Some sextupole correction is necessary at the highest fields. The basic feature of the design is a tapered pole with edge shims. Detailed comparison of the present design with that of Lari and Teng is a little difficult because some parameters are different in the two designs. Case 3 uses parameters which are close to their parameters. However, the overall dimensions differ slightly and the present design uses ∿ 10% more copper area. Perhaps the simplest statement that can be made is that the present design achieves somewhat better K curves than the crenellated case described by Lari and Teng.

As noted earlier, we were unable to alleviate the small tolerances on positioning the inner conductor. The reason for this appears to be the rather restrictive limits placed on the overall dimensions of the magnets.

In addition to the magnet designs described by Lari and Teng and by this report, a third B1 B2 design scheme has been investigated[7]. This third design used subsurface air holes in the outer regions of the pole tip for B1 and a reduced pole tip width for B2. During the progress of our work, NAL froze the coil window dimensions at values obtained from the third design in order to proceed with outer coil manufacture.

These values differ by a few tenths of an inch from our values. However, the third design has poorer high field performance than the design described in this report, so attempts will now be made to incorporate the tapered pole with edge shims into a design which uses the existing coil window. Initial results of this work[7] indicate high field performance which is very similar to that of the magnets described in our report.

Acknowledgements

It is a pleasure to acknowledge the extensive assistance of Mr. J.H. Dorst in this work. The N.A.L. Computer Center Staff, especially Miss A. Georgoulakis, were most helpful in the runs made remotely at N.Y.U. Similarily Mr. P. Rhodes and the L.R.L. Computer Center Staff were most cooperative in the runs made at Berkeley.

References

1. R.J. Lari and L.C. Teng, I.E.E.E. Trans. on Nuc. Science NS-16, No. 3,667 (1969).
2. LINDA was written by R.S. Christian (Purdue), J.H. Dorst (LRL), and T.P. Clements (LRL).
3. NAL Design Report, January, 1968.
4. D. Edwards, private communication.
5. R. Yamada, TM-171 0420, May 6, 1969.
6. R. Sheldon, private communication.
7. R. Yamada, private communication.
8. H.N. Henrichsen, et al, CERN Preprint ISR-MAG/66-12 (NAL Preprint No. 1688)
9. Taylor Lyman, et al, Editors, Metals Handbook (A.S.M., Metals Park, Ohio, 1961) Vol. 1 8th Edition p. 792.
10. For example:

    H.B. Dwight and C.F. Abt, Rev. Sci. Instr. 7, 144 (1936)

    M.E. Henderson and M.G. White, Rev. Sci. Instr. 9, 19 (1938)

    J.D. Howe and I. Walerstein, Rev. Sci. Instr. 9, 53 (1938)

    Simon Freed, Rev. Sci. Instr. 11, 117 (1940)

    Both Henderson et al and Howe et al refer to an unpublished pole taper derived by H.A. Bethe. Dr. R.R. Wilson has also noted the existence of this theoretical pole taper. Examples of tapered poles used in accelerators may be found in books on accelerator design, for example:

    M.S. Livingston and J.P. Blewett, Particle Accelerators (McGraw-Hill Book Company, Inc. 1962)

The following Russian reference describing the bending magnets in the beam transport system at Serpukhov is a recent example of magnet design using a tapered pole and edge shims --

A.V. Alekseev, M.D. Veselov, V.S. Kuznetsov, Yu.A. Lastochkin, I.A. Mozalevsky, A.V. Nikiforovsky, B.I. Tarasov, A.M. Frolov, IHEP, 68-62-K.

11. M.E. Rose, Phys. Rev. 53, 715 (1938).

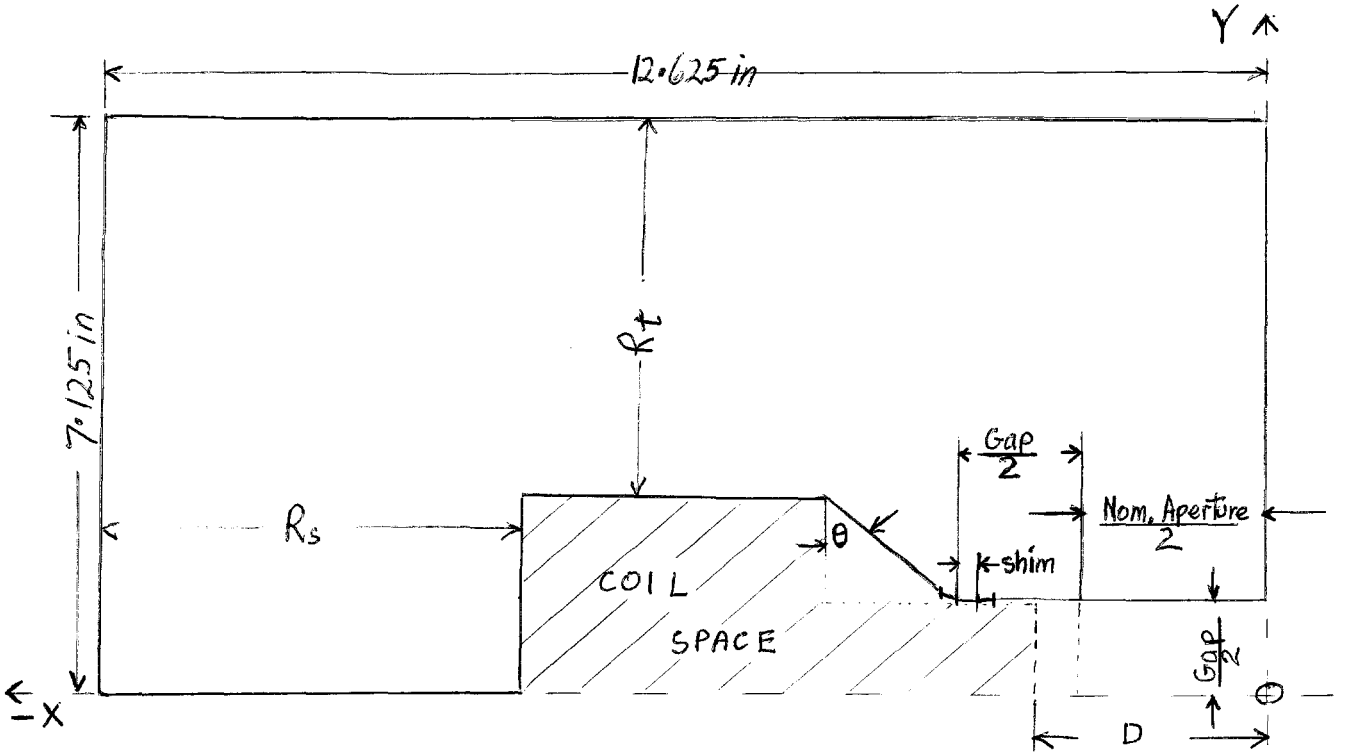

FIG. 1 STARTING POINT FOR MAGNET DESIGN.

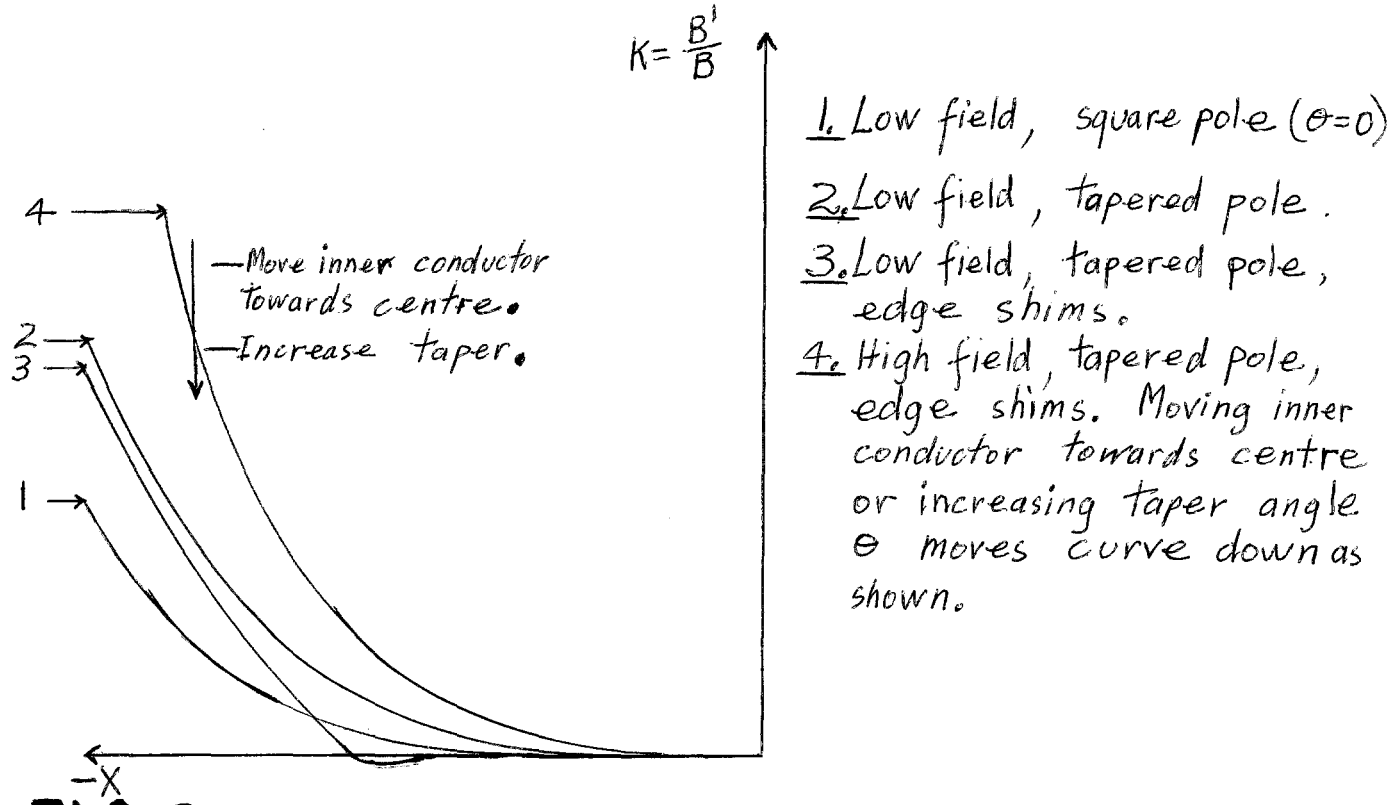

FIG. 2 K CURVE VARIATIONS.

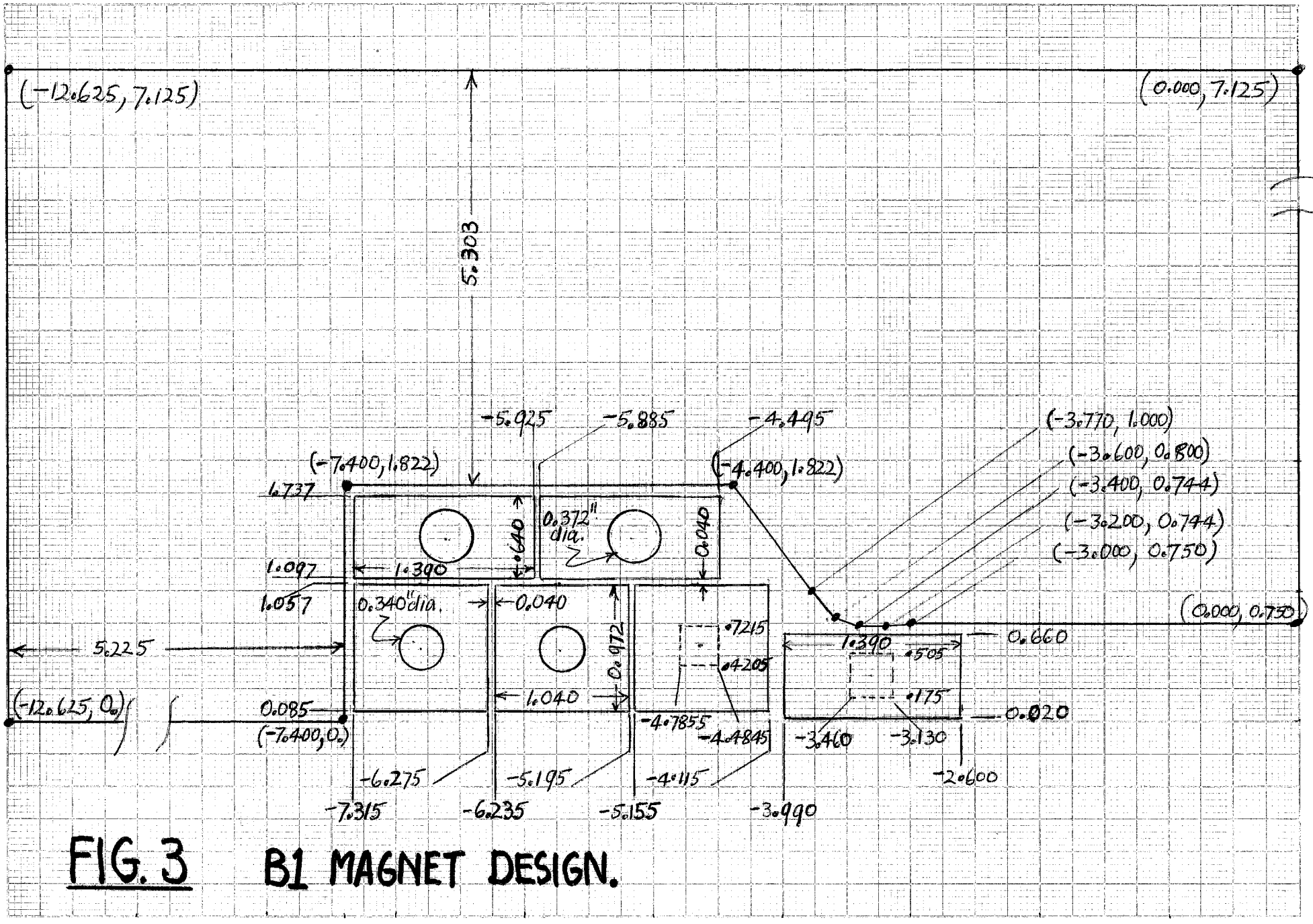

FIG. 3 B1 MAGNET DESIGN.

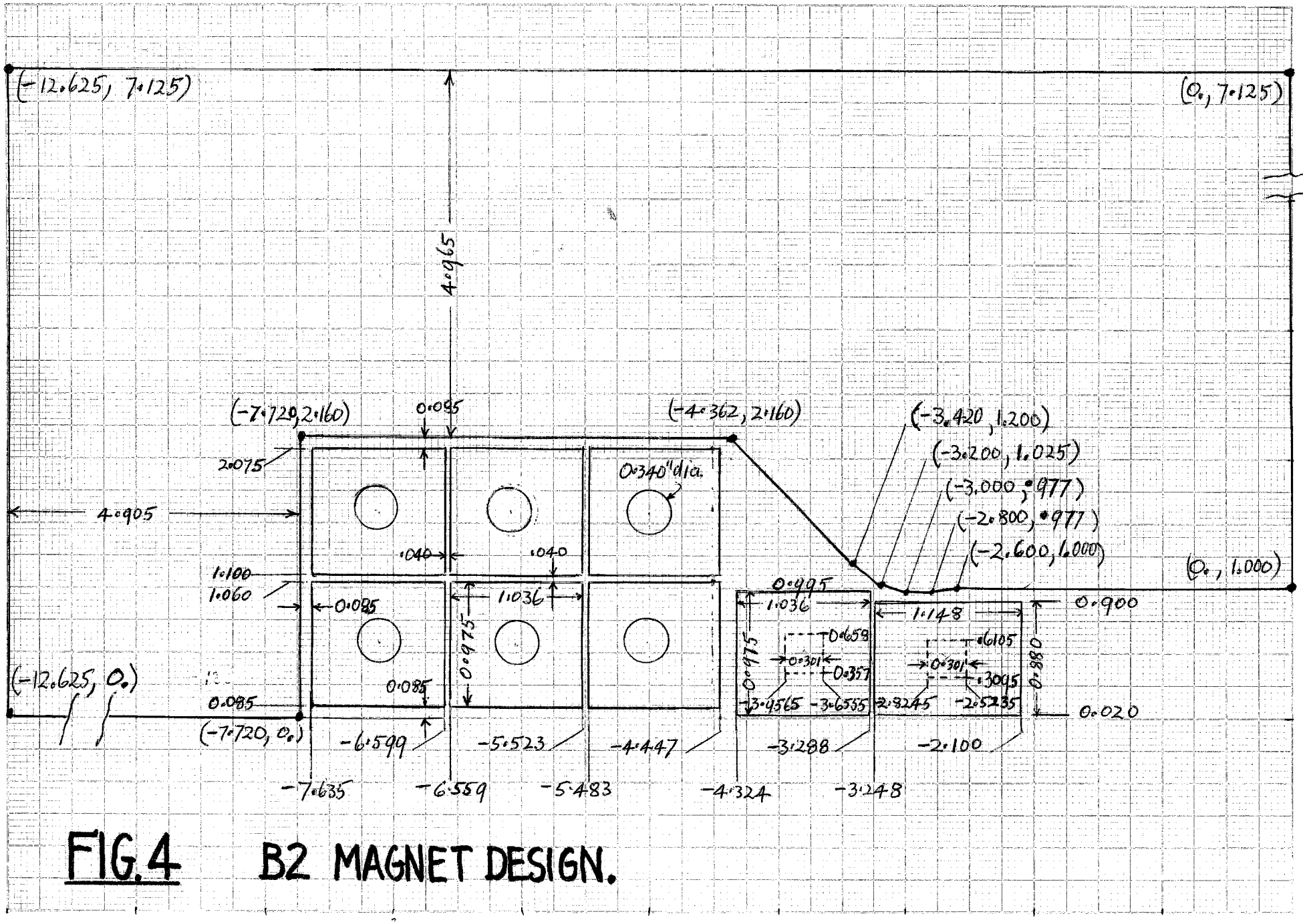

FIG. 4 B2 MAGNET DESIGN.

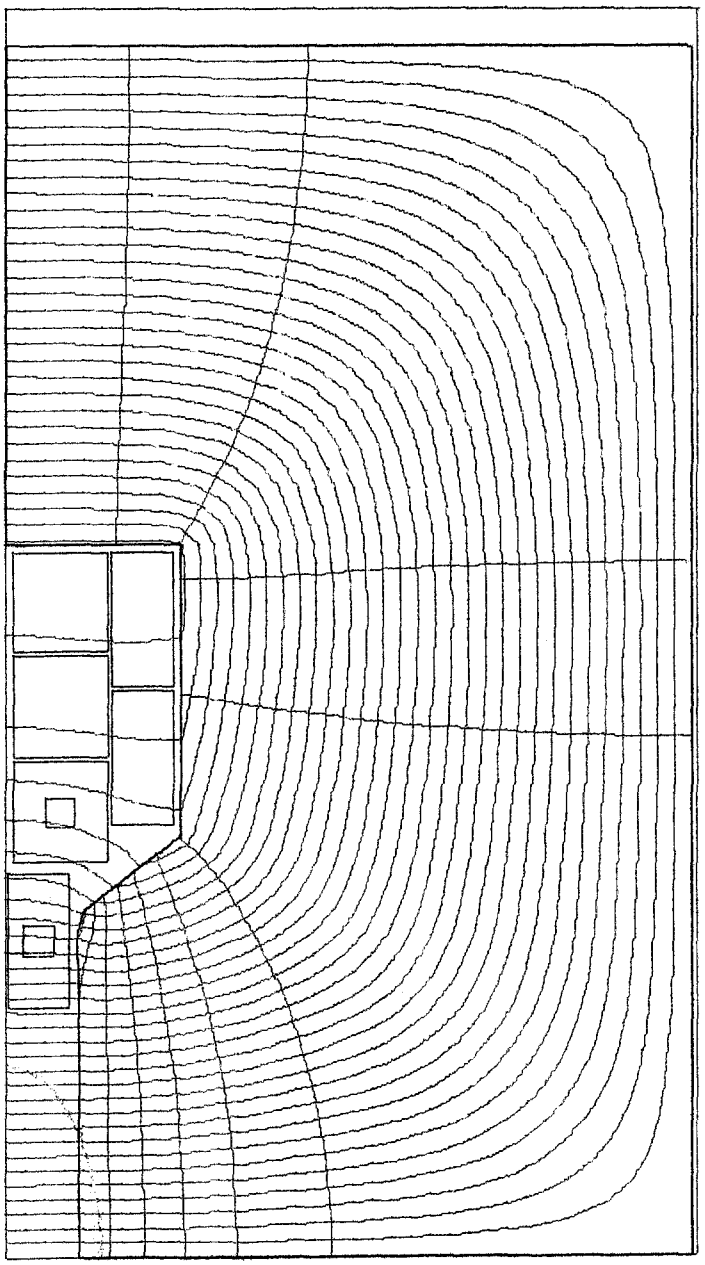

```
   134 CYCLE    5  TAPE   1822   VZERO =   0.
 2.1000 TESLAS      FILE    1     DELV =    .010000
AMPFAC = 1.0995                  AZERO =   0.
 11/25/69.    19.17.20.           DELA =    .200000
 X FROM     -13.000 TO       0.
 Y FROM       0.    TO       7.200
 SCALE FACTOR =     20.000
```

FIG. 5 B1 FLUX AND POTENTIAL LINES, 21 kgauss.

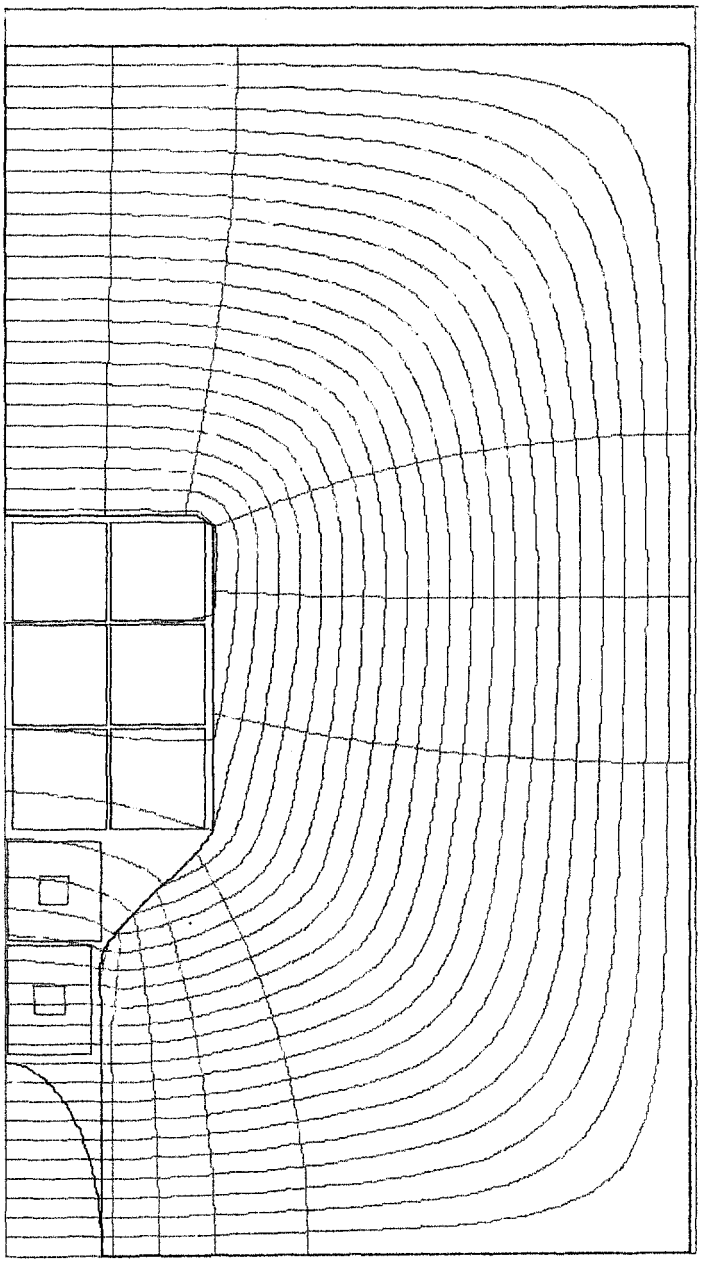

```
    119 CYCLE    6   TAPE   1822   VZERO =   0.
 2.1000 TESLAS       FILE    2      DELV =    .010000
AMPFAC = 1.0928                    AZERO =   0.
 11/22/69.    23.37.50.             DELA =    .200000
 X FROM     -13.000 TO       0.
 Y FROM       0.    TO       7.200
 SCALE FACTOR =     20.000
```

FIG. 6 B2 FLUX AND POTENTIAL LINES, 21 Kgauss.

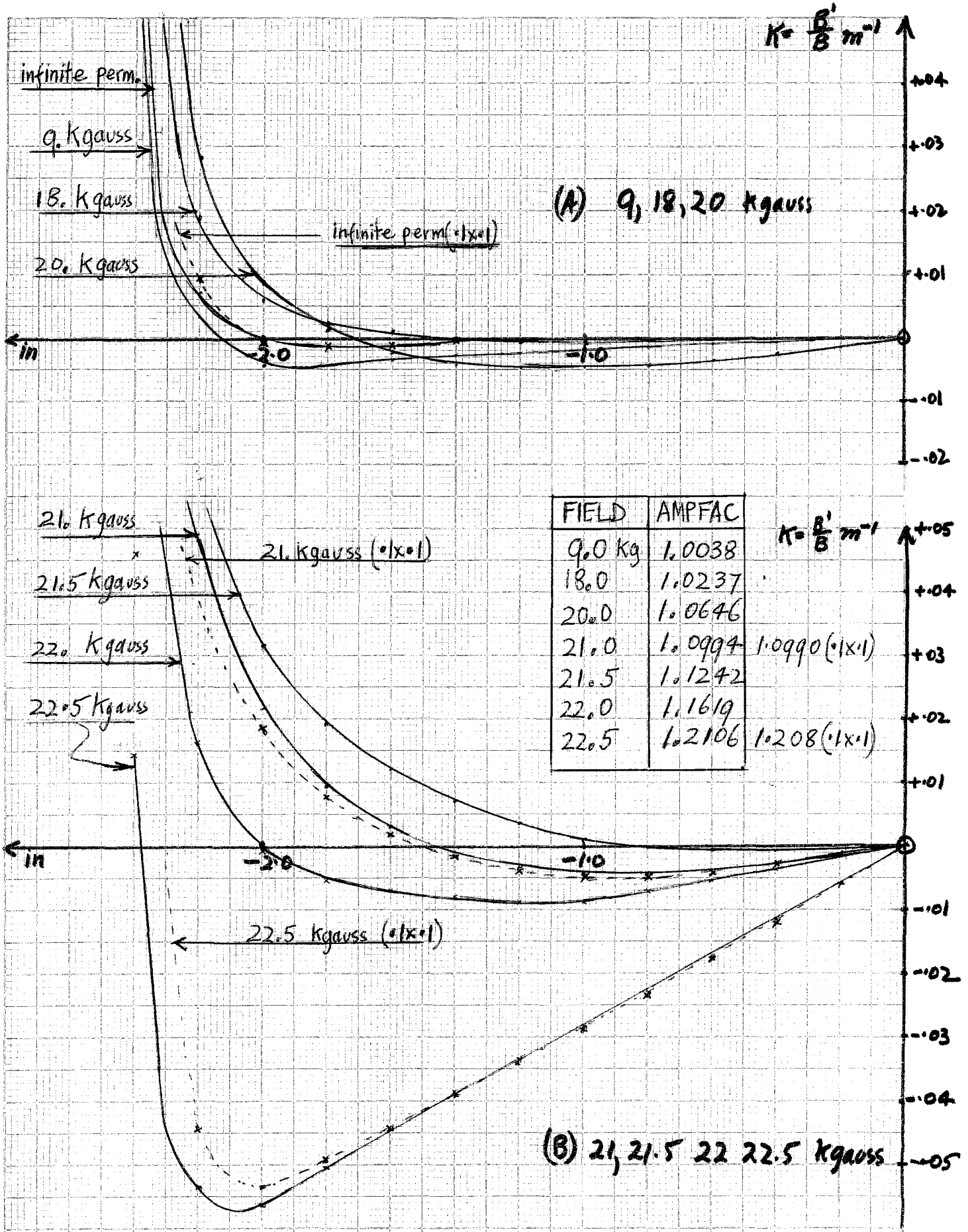

FIELD	AMPFAC	
9.0 Kg	1.0038	
18.0	1.0237	
20.0	1.0646	
21.0	1.0994	1.0990 (·1x·1)
21.5	1.1242	
22.0	1.1619	
22.5	1.2106	1.208 (·1x·1)

FIG. 7 B1 MAGNET, STACKING FACTOR 0.99, LINDA IRON

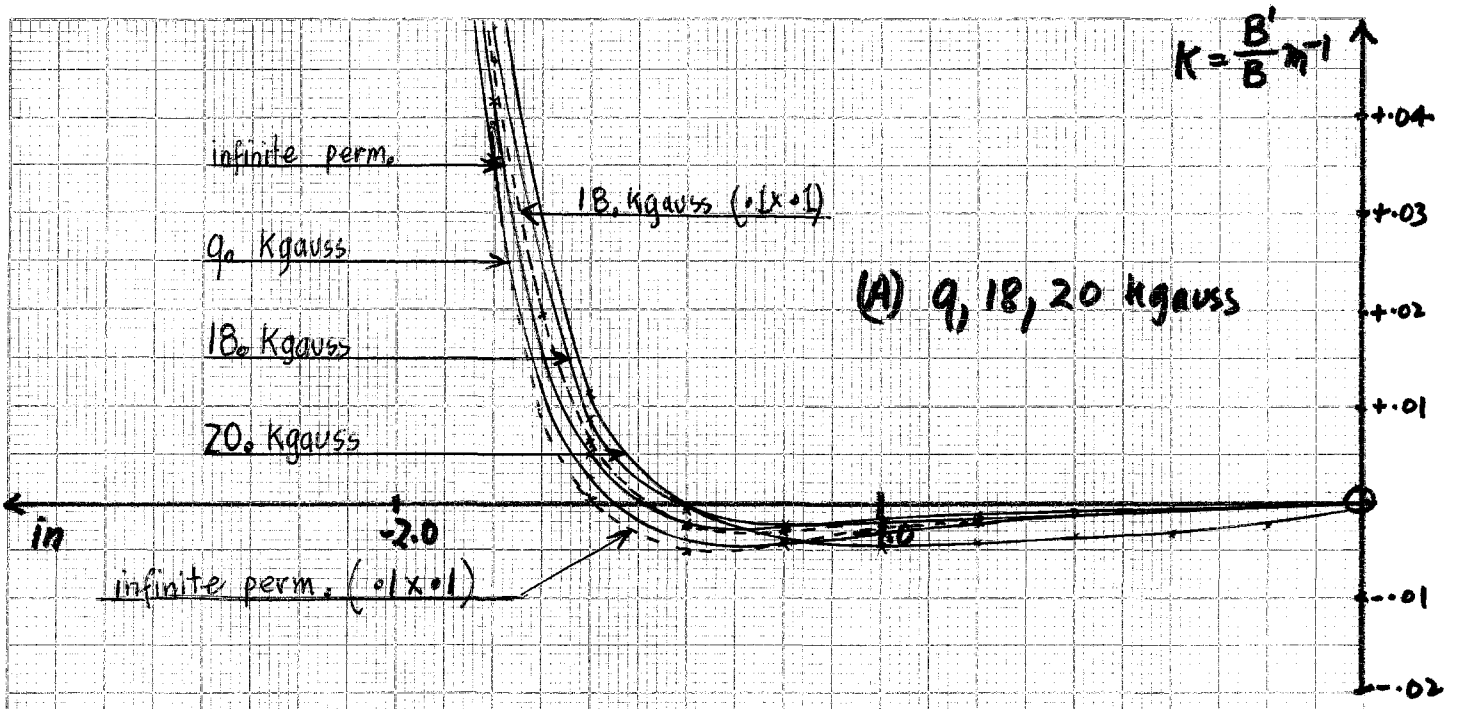

FIELD	AMPFAC	
9.0 Kg	1.0031	
18.0	1.0227	1.0230 (.1x.1)
20.0	1.0618	
21.0	1.0927	1.0935 (.1x.1)
21.5	1.1138	
22.0	1.1441	
22.5	1.1830	1.1839 (.1x.1)

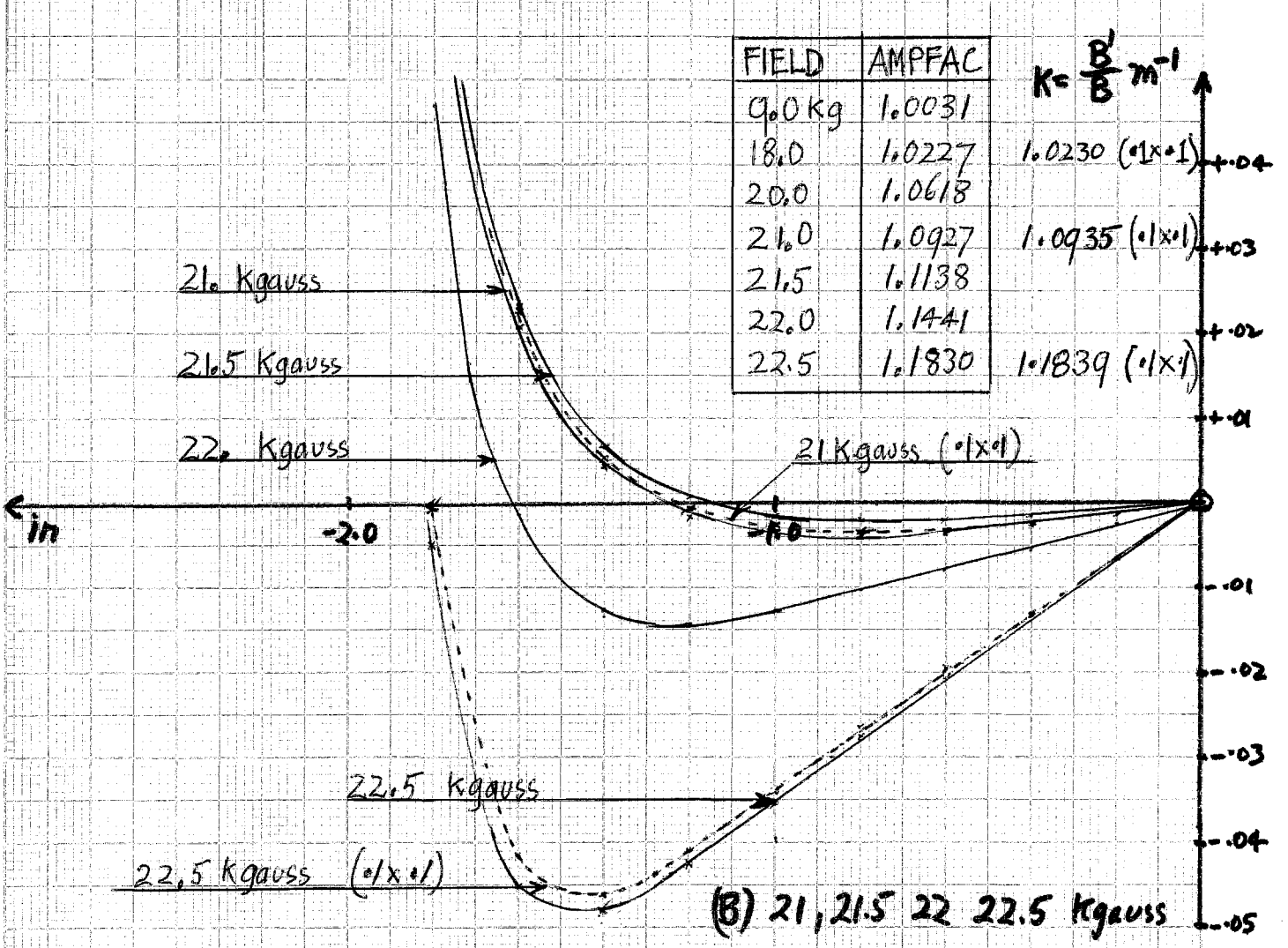

FIG. 8A B2 MAGNET, STACKING FACTOR 0.99, LINDA IRON

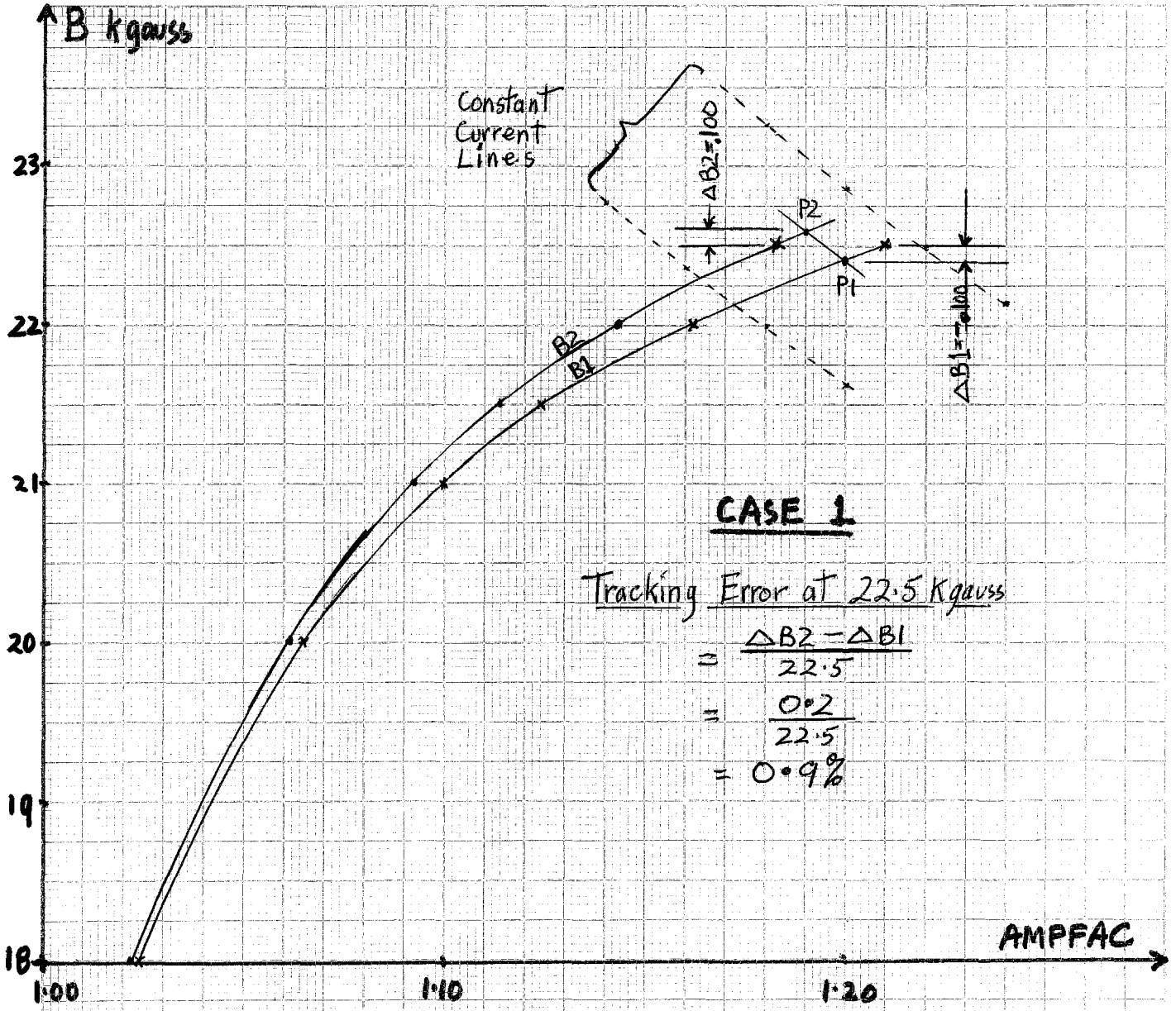

FIG. 8B. DETERMINATION OF B1-B2 TRACKING ERROR

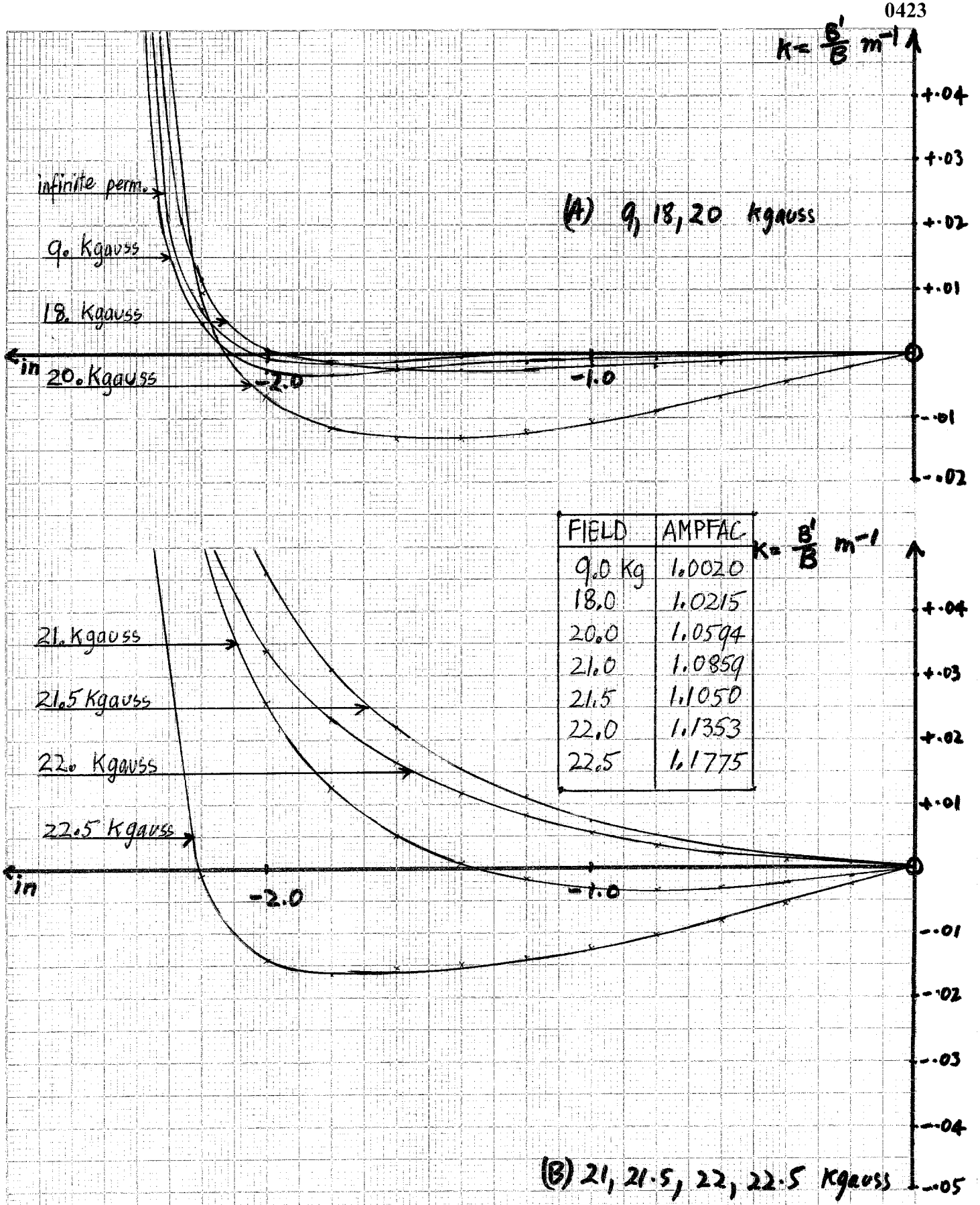

FIELD	AMPFAC
9.0 Kg	1.0020
18.0	1.0215
20.0	1.0594
21.0	1.0859
21.5	1.1050
22.0	1.1353
22.5	1.1775

FIG. 9 B1 MAGNET, STACKING FACTOR 0.99, TEST IRON.

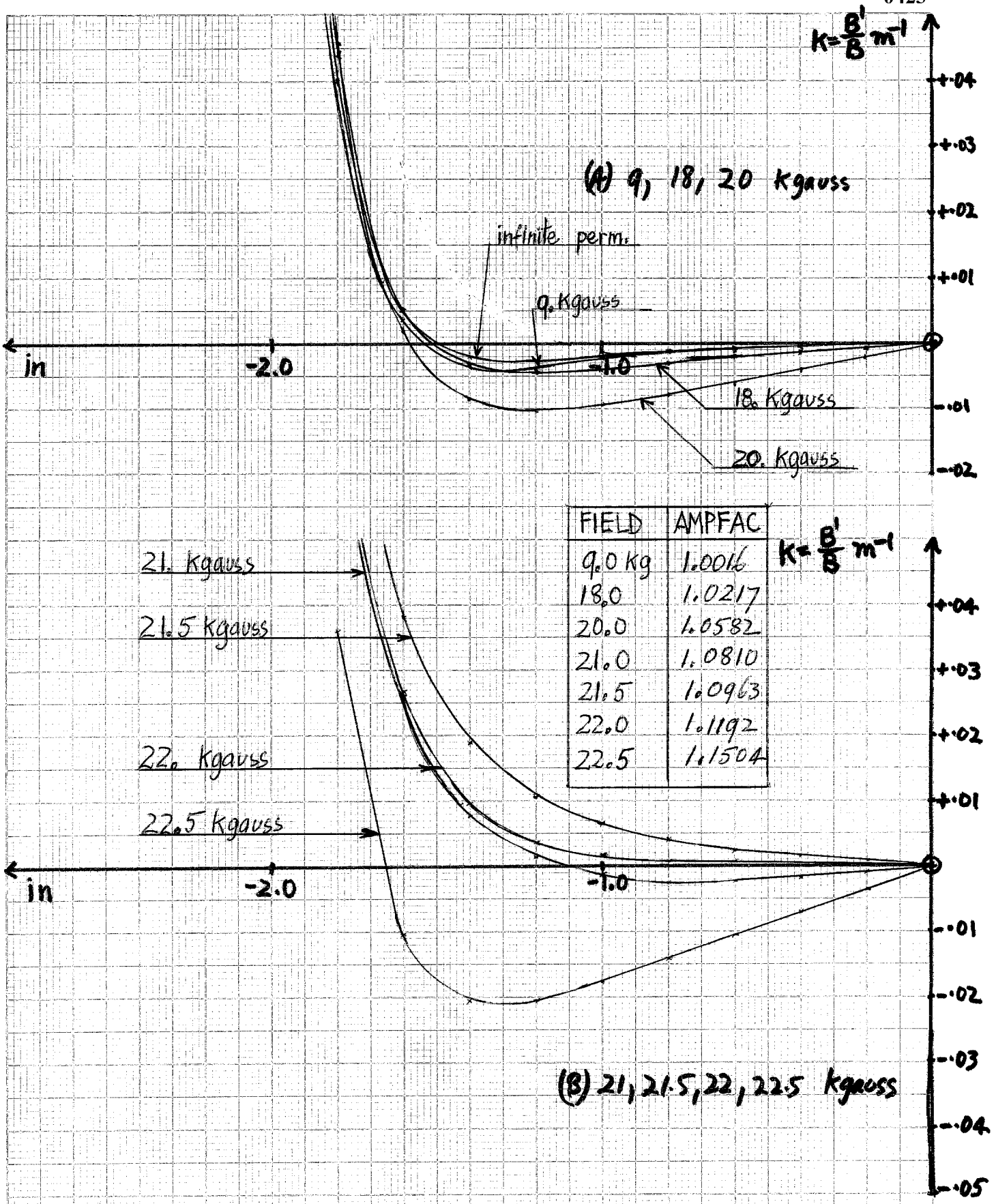

FIELD	AMPFAC
9.0 kg	1.0016
18.0	1.0217
20.0	1.0582
21.0	1.0810
21.5	1.0963
22.0	1.1192
22.5	1.1504

FIG. 10 B2 MAGNET, STACKING FACTOR 0.99, TEST IRON.

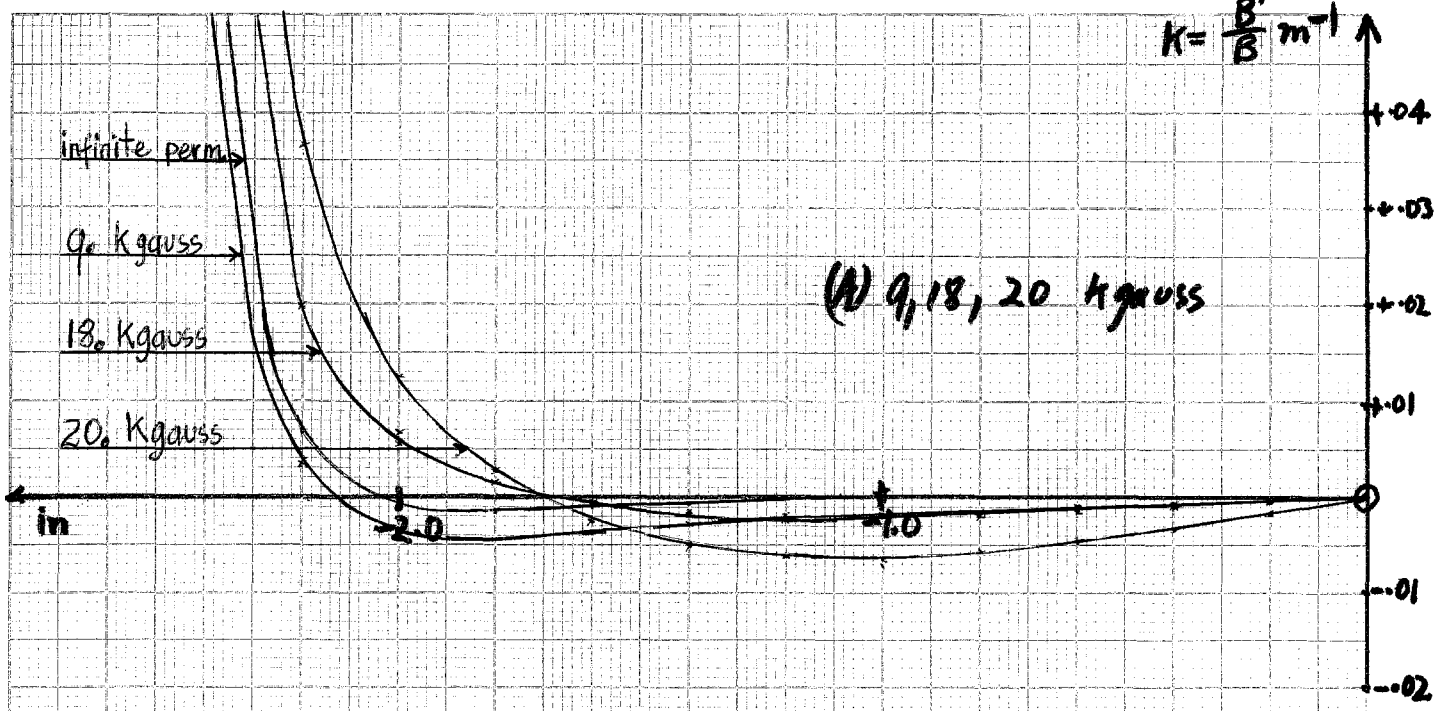

FIELD	AMPFAC
9.0 kg	1.0040
18.0	1.0329
20.0	1.0875
21.0	1.1385
21.5	1.1830
22.0	1.2380
22.5	1.3024

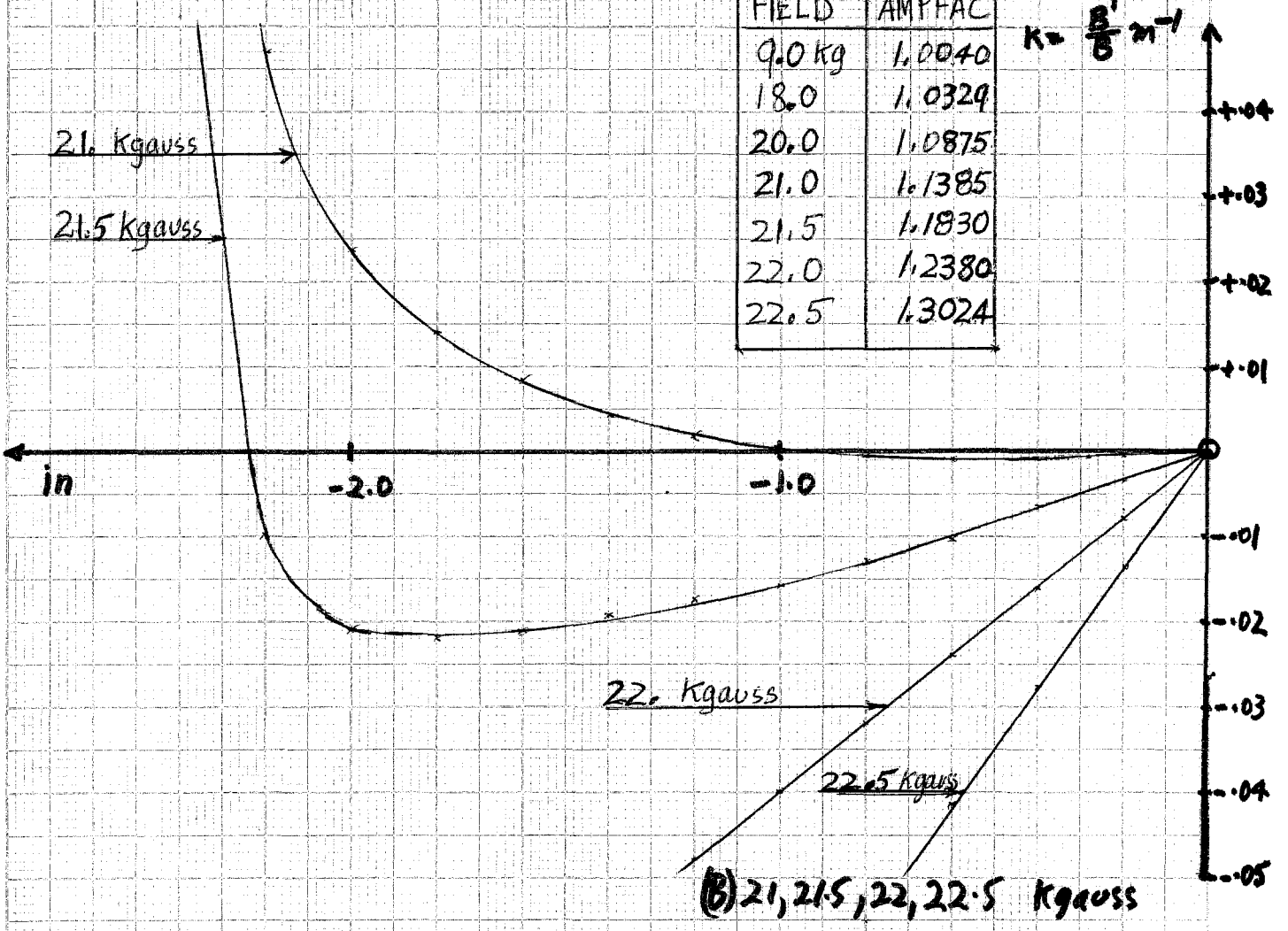

FIG. 11 B1 MAGNET, STACKING FACTOR 0.96, LINDA IRON

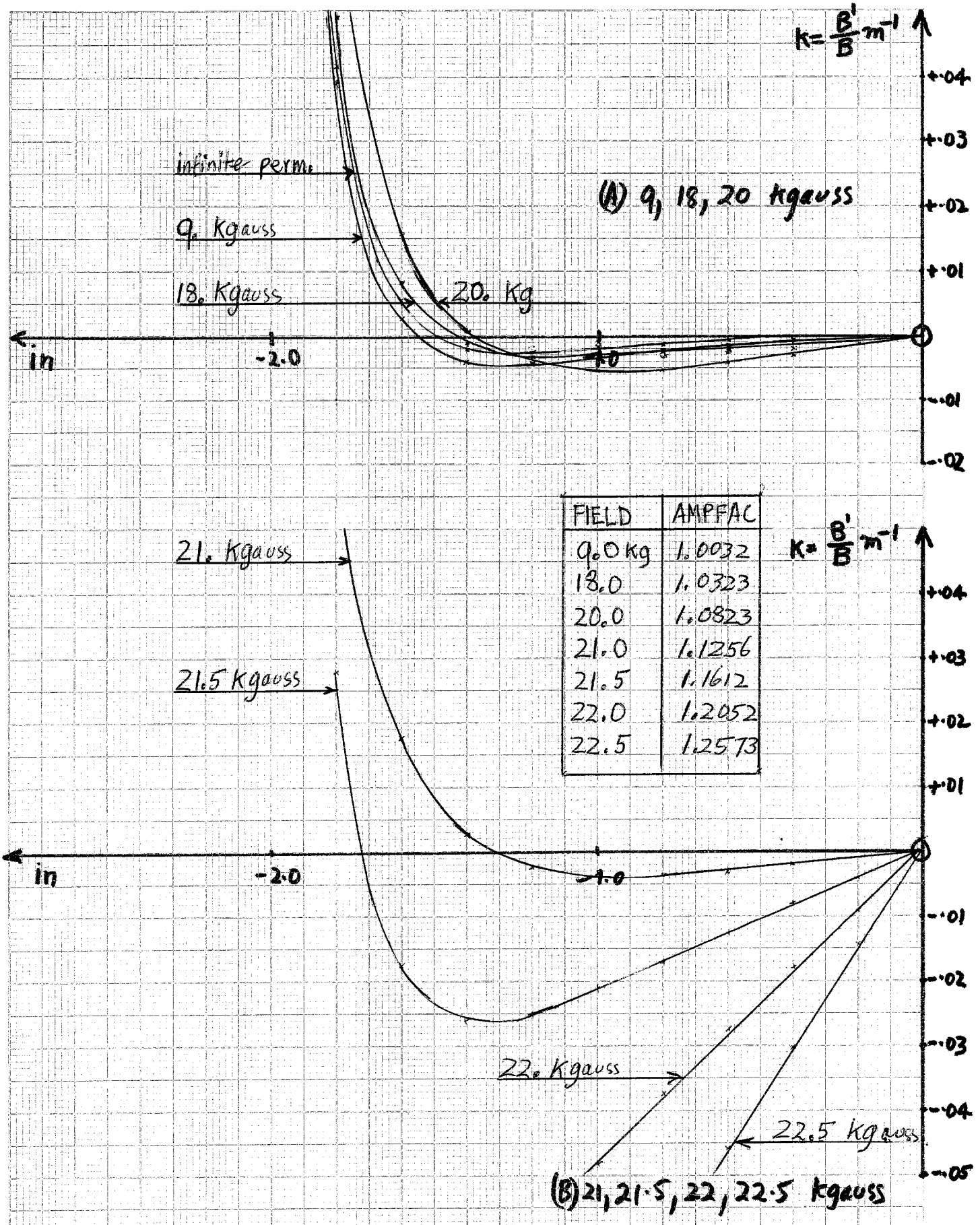

FIELD	AMPFAC
9.0 kg	1.0032
18.0	1.0323
20.0	1.0823
21.0	1.1256
21.5	1.1612
22.0	1.2052
22.5	1.2573

FIG. 12 B2 MAGNET, STACKING FACTOR 0.96, LINDA IRON